Case Studies in Thermal Engineering 55 (2024) 104125

Contents lists available at ScienceDirect

Case Studies in Thermal Engineering

journal homepage: www.elsevier.com/locate/csite

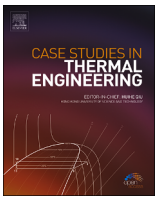

Numerical study and optimization of thermal efficiency for a pin fin heatsink with nanofluid flow by modifying heatsink geometry

Behzad Heidarshenas [a], Awatef Abidi [b], S. Mohammad Sajadi [c], Yanjie Yuan [a, *], A.S. El-Shafay [d, e], Hikmet Ş. Aybar [f, g, **]

[a] College of Mechanical and Electrical Engineering, Nanjing University of Aeronautics and Astronautics, China
[b] Physics Department, College of Sciences Abha, King Khalid University, Saudi Arabia
[c] Department of Nutrition, Cihan University-Erbil, Kurdistan Region, Iraq
[d] Department of Mechanical Engineering, College of Engineering in Al-Kharj, Prince Sattam bin Abdulaziz University, Al-Kharj, 11942, Saudi Arabia
[e] Mechanical Power Engineering Department, Faculty of Engineering, Mansoura University, Mansoura, 35516, Egypt
[f] Department of Mechanical Engineering, Eastern Mediterranean University, Famagusta, TRNC, via Mersin 10, Turkey
[g] Department of Medical Research, China Medical University Hospital, China Medical University, Taichung, Taiwan

ARTICLE INFO

Keywords:
Thermal resistance
Temperature uniformity
Heatsink
Two-phase nanofluid
Machine learning

ABSTRACT

This paper presents a numerical study on the thermal efficiency of a pin fin heatsink (HEK). The working fluid used is an alumina/water nanofluid, which enters the HEK in a laminar flow regime and exits from its surroundings. This study involves varying the distance between circular pin fins, their height, and their diameter. By altering these parameters, we determine the values of thermal resistance (THR) and temperature uniformity (Teta) on the HEK, along with the heat transfer coefficient (HTC). We further optimize the obtained results using artificial intelligence techniques to minimize the THR of the HEK, maximize the HTC, and achieve the best Teta on the HEK. This numerical investigation employs a two-phase approach to model nanofluid flow within the HEK. The optimization process yields predictions with an accuracy of less than 4%. The findings reveal that increasing the height of the pin fins reduces the HTC and the heat capacity of the HEK, while simultaneously improving the Teta on the HEK. Expanding the distance between pin fins enhances the HTC, decreases the THR of the HEK, and further improves the Teta on the HEK. Similarly, augmenting the diameter of the pin fins amplifies the HTC, reduces the THR, and enhances the Teta on the HEK.

Nomenclature

a	Acceleration (m^2/s)
A	Constant
B	Constant
C	Constant
Cp	Specific heat (J/kg.K)
d	Pin diameter (mm)

* Corresponding author.
** Corresponding author. Department of Mechanical Engineering, Eastern Mediterranean University, Famagusta, TRNC, via Mersin 10, Turkey.
E-mail addresses: yanjieyuan@nuaa.edu.cn (Y. Yuan), hikmet.aybar@emu.edu.tr (H.Ş. Aybar).

https://doi.org/10.1016/j.csite.2024.104125
Received 3 October 2023; Received in revised form 5 January 2024; Accepted 11 February 2024
Available online 12 February 2024

d_p	Nanoparticles diameter (nm)
g	Gravitational acceleration (m^2/s)
h	Heat transfer coefficient ($W/m^2.K$)
L	Pin length (mm)
HEk	Heat sink
k	Thermal conductivity ($W/m.K$)
N	Number of experiments
p	Pressure (Pa)
Pr	Prandtl number
Re	Reynolds number
T	Temperature (K)
Teta	Temperature uniformity ($\frac{T_{Max}-T_{min}}{q''}$) ($m^2.K/W$)
THR	Thermal resistance ($\frac{T_{Mid}-T_{in}}{q''}$) ($m^2.K/W$)
v	Velocity (m/s)
V_B	Brownian velocity of nanoparticles
w	Pin distance (mm)

Greek symbols

φ	Solid volume fraction
μ	Dynamic viscosity ($kg/m.s$)
α	Thermal diffusivity (m^2/s)
β	Thermal expansion coefficient
ρ	Density kg/m^3)
(δ	Distance between particles
α_i	unknown coefficients

Subscripts

f	Fluid
m	Mixture
p	Particle

1. Introduction

A large number of investigations are conducted yearly in applied industries due to the extensive use of HEKs in the fields. Researchers are interested in HEKs because of their many uses and significance to companies [1,2]. The goal of this research is to modify the shape of HEKs to increase their thermal efficiency. On the other hand, researchers have recently shown a lot of interest in the usage of nanofluids [3,4]. Nowadays, many researchers employ nanotechnology, which is one of the most important fields in heat transfer (HTF) [5,6]. They use nanofluids in HEKs to improve their thermal efficiency [7,8]. HEKs have different shapes and many researchers publish their publications in the field [9]. Alihosseini et al. [10] reviewed the effect of geometry on HEK thermal performance. Liquid coolants are being used more and more in personal computers, laptops, servers, and supercomputers as a result of technological advancements and the downsizing of electronic systems. Micro HEKs are often used to accelerate cooling. The performance of HEKs in terms of HTF is greatly influenced by proper geometric design. They reviewed articles in the field using three approaches: (1) flow patterns approach, (2) cross-sectional geometry approach, and (3) inlets and outlets with different cross-sections. Ghaneifar et al. [11] examined the hybrid nanofluid flow inside a foam-copper layered HEK. The HEK was composed of several layers that were under constant heat flux. In the two suggested models, they tried to develop an appropriate HEK with the ideal thickness of porous layers to increase HTF and reduce pressure drop. They considered dimensionless numbers to assess the performance evaluation criteria (PEC) to evaluate favorable (HTF) and unfavorable (pressure drop) results. The influence of the thickness of each layer of the porous media on thermo-hydraulic parameters such as friction coefficient, Nusselt number (Nu), and PEC was examined using computational fluid dynamics (CFD). Their results revealed that the use of porous layers significantly improves HTF and the maximum PEC corresponds to a volume percentage (φ) of 0.1.

HEKs are widely utilized for the thermal management of many devices, such as solar panels, batteries, electronic devices, etc [12,13]. Nowadays, the operation of many devices depends on the presence of HEKs, and the absence of HEKs can cause serious damage to them [14,15]. The heat generation in many devices, such as electronic components, sub-processors, graphics cards, etc., as well as some types of batteries such as lithium-ion batteries, has made researchers improve the thermal efficiency of HEKs [16,17]. Various types of fluids such as water, ethylene glycol, air, etc. are used as cooling fluids in HEKs [18,19]. Today, due to the better efficiency of nanofluids compared to the mentioned fluid, many researchers employ nanofluids in HEKs [20,21]. Nanotechnology is utilized in many industries, such as heat exchangers. One of the important things in a HEK is its fabrication, which should be economical and cost-effective. The use of pin fins to improve the thermal efficiency of HEKs is effective in terms of heat and fabrication. Many studies have been conducted in the field of using pin fin heat sink [22–25]. Metzger et al. [26] experimentally investigated the effect of pin fin geometry on improving the performance of internal airfoil coolers. First, a bunch of pins with circular sections with different orientations was used. Then pins with rectangular sections were examined. Their results showed that circular pins with stepped and

linear arrangements can increase heat transfer and reduce pressure drop in some cases. Using long pins increases heat transfer, but increases pressure drop. In another study, Metzger and Aley [27] investigated the type of pins. Yu et al. [28] investigated a plate-pin fin heat sink and compared its results with the plate fin heat sink. Their results showed that the thermal resistance of a plate-pin fin heat sink was about 30% lower than the plate fin heat sink used to make a plate-pin fin heat sink under the condition of the same wind speed. Ali Hussein [29] numerically investigated the heat transfer inside a pin-fin microchannel by examining the rectangular shape of the pins. He used the finite element method to solve partial differential equations for the simulation of laminar flow and used water as a single-phase fluid in cooling. His results showed that the increase in the mass flow rate led to an increase in the average Nusselt number, pressure drop, and performance index while reducing the average thermal resistance. Therefore, many HEKs have been designed by researchers using pin fins. In this article, a novel design of a HEK with circular pin fins is thermally analyzed. Inside the HEK, several pin fins are used, and the fluid flows through them. Nanofluid is also used in the HEK to improve its performance. For a better analysis, the heatsink Teta, THR, HTC, and pressure drop are assessed by changing the diameter and height of the pin fins and their distance using machine learning.

2. Definition of the problem

The HEK is circular, where the laminar alumina/water nanofluid flow enters from the middle of the HEK ($T_{in} = 293K, Re = 300$) and exits from its surroundings ($p_{out} = 1atm$). Its height is 15 mm and a large number of circular pin fins are placed in it. Heat flux enters it from under the heatsink and the upper part of the heatsink is insulated. Pins with specific lengths and heights are located on the heatsink at a distance from each other as seen in Table 1. Fig. 1 illustrates a schematic of a part of the HEK and presents the thermophysical properties of the nanofluid.

2.1. Governing equations for nanofluid two-phase flow

The governing equations for nanofluid flow are expressed as follows using the two-phase mixture method for steady flow and Newtonian and incompressible fluid [31]:

$$\nabla \cdot \left(\rho_m V_m\right) = 0 \tag{1}$$

$$\nabla \cdot \left(\rho_m V_m V_m\right) = -\nabla p + \nabla . \left(\mu_m \nabla V_m\right) + \nabla . \left(\sum_{k=1}^{n} \varphi_k \rho_k \, V_{dr,k} V_{dr,k}\right) - \rho_{m,i} \beta_m g \left(T - T_i\right) \tag{2}$$

$$\nabla . \sum_{k=1}^{n} \left(\rho_k \, c_{Pk} \varphi_k V_k T\right) = \nabla . \left(k_m \nabla T\right) \tag{3}$$

$$\nabla . \left(\varphi_p \rho_p \, V_m\right) = -\nabla . \left(\varphi_p \rho_p \, V_{dr,p}\right) \tag{4}$$

where V_m is expressed as follows [32]:

$$V_m = \frac{\sum_{k=1}^{n} \varphi_k \rho_k \, V_p}{\rho_m} \tag{5}$$

and $V_{dr,k}$ is obtained as

$$V_{dr,k} = V_k - V_m \tag{6}$$

$$V_{pf} = V_p - V_f \tag{7}$$

$$V_{dr,p} = V_{pf} - \sum_{k=1}^{n} \frac{\varphi_k \rho_k}{\rho_m} \, V_{fk} \tag{8}$$

Finally, according to the equations of Manninen et al. [33] and Schiller and Naumann [34]:

Table 1
Variables related to the geometry of the pins and their change interval.

Parameter	Start	Finish
Pin length L (mm)	5	15
Pin distance w (mm)	10	15
Pin diameter d (mm)	1	4

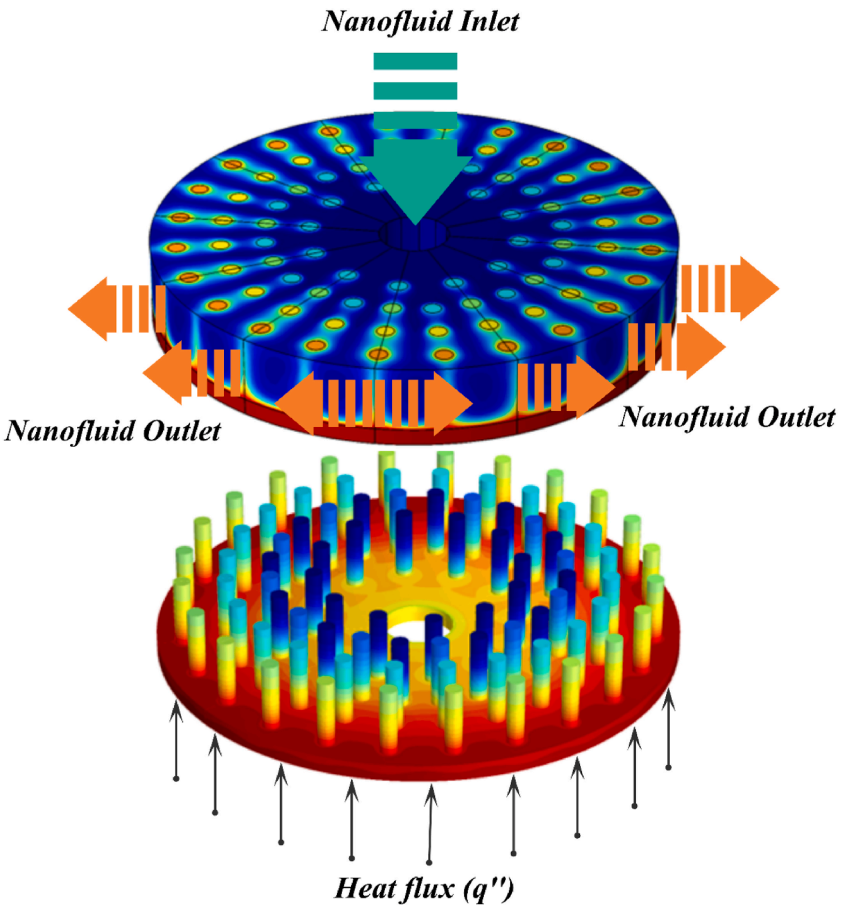

	$k\ (W/m.K)$	$\rho\ (kg/m^3)$	$\mu\ (kg/m.s)$	$C_P\ (J/kg.K)$
Water	0.613	997.1	0.001	4179
Al_2O_3	40	3970	-	765

Fig. 1. A schematic of the HEK and the properties of nanoparticles and water [30].

$$V_{pf} = \frac{\rho_p\, d_p^2}{18\mu_f f_{drag}} \frac{\left(\rho_m - \rho_p\right)}{\rho_P} a^* \tag{9}$$

$$f_{drag} = \begin{cases} 1 + 0.15\, Re_p^{0.687}, & Re_P \le 1000 \\ 0.0183 Re_P, & Re_P > 1000 \end{cases} \tag{10}$$

$$a^* = g - \left(V_m \cdot \nabla\right) V_m \tag{11}$$

The properties of nanofluid are obtained using the following relations [35]:

$$\rho_m = (1-\varphi)\,\rho_f + \varphi\rho_p \tag{12}$$

$$\beta_m = \left[\frac{1}{1+\frac{(1-\varphi)\rho_f}{\varphi\rho_p}}\frac{\beta_p}{\beta_f} + \frac{1}{1+\frac{\varphi}{1-\varphi}\frac{\rho_p}{\rho_f}}\right]\beta_f \tag{13}$$

Viscosity is calculated using the relation proposed by Masoumi et al. [36]:

$$\mu_m = \mu_f + \frac{\rho_p\, V_B d_p^2}{72C\delta} \tag{14}$$

where V_B and δ are the Brownian velocity of nanoparticles and the distance between particles, respectively, which can be obtained as follows:

$$V_B = \frac{1}{d_P}\sqrt{\frac{18k_BT}{\pi\rho_p d_p}} \tag{15}$$

$$\delta = \sqrt[3]{\frac{\pi}{6\varphi}}d_p \tag{16}$$

Constants are obtained as

$$C = \mu_f^{-1}\left[\left(c_1 d_p + C_2\right)\varphi + \left(c_3 d_p + C_4\right)\right] \tag{17}$$

$$C_1 = -0.000001133, C_2 = -0.000002771, C_3 = 0.0000009, C_4 = -0.000000393 \tag{18}$$

The thermal conductivity is determined using the correlation introduced by Chon et al. [37]:

$$\frac{k_m}{k_f} = 164.7\varphi^{0.7460}\left(\frac{d_f}{d_p}\right)^{0.3690}\left(\frac{k_p}{k_f}\right)^{0.7476} Pr_f^{0.9955} Re_f^{1.2321} \tag{19}$$

$$Pr_f = \frac{\eta}{\rho_f \alpha_f} \tag{20}$$

$$Re_f = \frac{\rho k_B T}{3\pi\eta^2\lambda_f} \tag{21}$$

$$\eta = A.10^{\frac{B}{T-C}}, A = 2.414\times10^{-5}, B = 247.8, C = 140 \tag{22}$$

2.2. Numerical method and optimization

In this paper, a numerical method is used to solve the problem. Numerical methods have been a technique for solving problems. The finite element method (FEM) is used to analyze partial and full differential equations to study the behavior of linear and nonlinear systems in one-, two-, and three-dimensional issues. The geometry of the problem is first drawn, and then the geometry is divided into several different elements. The elements are generated on the entire geometry, and the equations are solved on these elements. Since the physical system is divided into elements and nodes, all external and internal forces and specific parameters must be converted into elements and nodes. The calculations are numerical and their error rate is very important; hence, at least two sources of error are generated. Firstly, the solution for elements does not exactly match its actual values. More suitable elements lead to fewer calculation errors. Fortunately, many solutions become more accurate by reducing the element size. The next error is due to the simplifications of the algebraic equation. The governing equations become simpler, creating some errors. It should be remembered that solving FEM is highly dependent on computers and computer programming, and the conditions governing computers and the methods used in the process of solving them to perform calculations should not be ignored. The FEM is conceptually simple and is used for a wide range of two- and three-dimensional problems. The steps for solving the problem in the FEM method are given in Fig. 2.

In this paper, the response surface method is utilized for the optimization and statistical modeling of data. In the statistical method, the interpretation and determination of parameters are based on the response factors to determine the optimal values. Therefore, the response surface is a method for designing experiments, regression analysis, and calculating optimal values. This method is employed in cases where there are certain controllable and effective factors. The geometrical parameters of the HEK are assessed and sensitivity analysis is performed, and then, the optimal parameters are presented. The aim of using this method is to estimate the optimal conditions and determine the values for the effective parameters to find the region and position where all the responses are optimal. The other goal is to create a communication model between the input factors and the outputs. One of the necessary steps before using response surface methods is to choose a suitable experimental design. Designs such as factorial can only be used for first-order

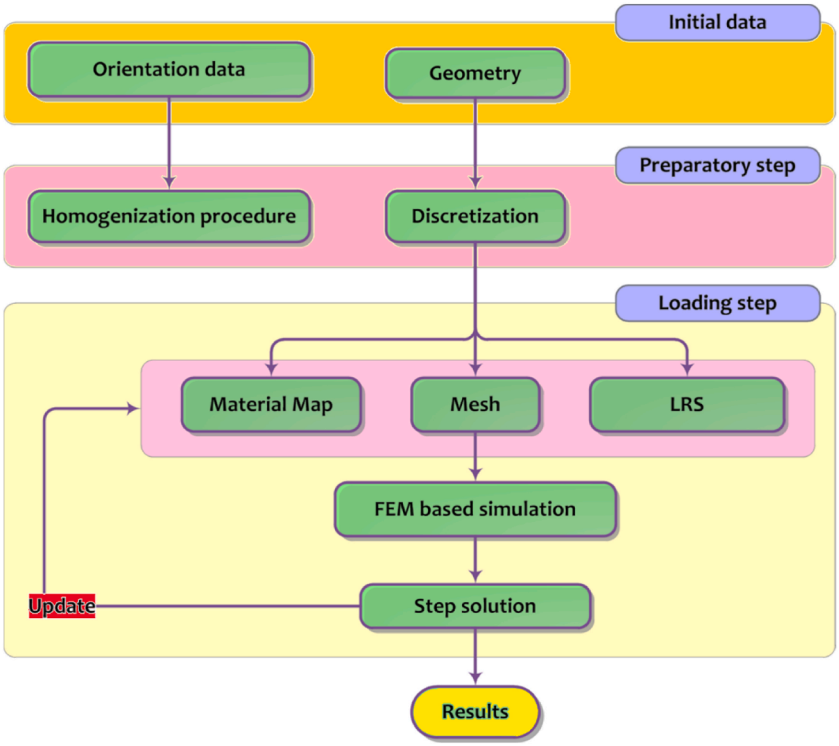

Fig. 2. Steps of solving equations using the FEM method.

and linear models. However, concerning the data that is a quadratic function, one should utilize the plans provided by the response surface method such as the central composite design (CCD).

The CCD method that was developed by Box-Wilson is employed in this study. This method can estimate the curvature well. This approach typically uses five surfaces, however face-centered CCD may transform it into a three-surface method, which is often used in engineering computations. The effective parameters and their change interval must be determined initially.

As a result, three components are identified at three different points throughout their change period. These settings take into account two different actual and coded symbol kinds. You can see that the beginning, middle, and end of the range of changes in the factors are defined in the surface column. The following polynomial function may be used in this manner to produce the mathematical dependence:

$$Response = \alpha_0 + \sum_{i=1}^{3} \alpha_i x_i + \sum_{i=1}^{3} \alpha_{ii} x_i x_i + \sum_{i=1}^{3} \sum_{j=1, j\neq i}^{3} \alpha_{ij} x_i x_j \tag{23}$$

where α_0, α_i, α_{ii}, and α_{ij} are unknown coefficients that are determined by the response surface method.

By examining the P-value, Fisher statistics along with R^2 and $R^2_{adjusted}$, the quality of the models can be evaluated. The larger R^2, which is the evaluation coefficient of the regression model, indicates that the model is more successful in predicting the dependent variable. The following relations can be used to calculate these coefficients [38]:

$$R^2 = \frac{\text{Explained sum of squares}}{\text{Total sum of squares}} = 1 - \frac{\text{Residual sum of squares}}{\text{Total sum of squares}} \tag{24}$$

$$R^2_{adjusted} = 1 - \frac{\left(1 - R^2\right)(N-1)}{N - P - 1} \tag{25}$$

where P is the number of prediction variables and N is the total number of experiments. In the model, terms having an F-value below 1 are eliminated [39]. Thus, B^2 terms are removed from the Teta and the THR relations. Also, only terms L^2 and B^2 are removed in Be relation. As a consequence, the regression equation is made simpler and it is easier to predict the outcomes.

2.3. Grid study and validation

To generate the grid on the HEK, the number of elements is different for different geometries due to the presence of pin fins and the changes in their distance and dimensions. In Table 2, the values of THR and Teta are shown in the intermediate values of the vari-

Table 2
The number of elements and their effect on the THR and Teta of the HEK.

No. of elements	Teta (m^2.K/W)	Deference (%)	R (m^2.K/W)	Deference (%)
372596	0.00064	17.9%	0.00040	29.8%
432967	0.00073	6.4%	0.00051	10.5%
535183	0.00078	0	0.00057	0
613737	0.00078	0	0.00057	0

ables for the grids with different elements. Other grid studies experience the same results. An example of a HEK grid is illustrated in Fig. 3.

An experimental and numerical work by Aghakhani et al. [40] is used to verify the results. In this article, a circular HEK was utilized and the effect of nanofluid flow was evaluated. They carried out the thermal analysis of aluminum and copper HEKs. Table 3 compares the temperature values of the water in the copper HEK obtained from the present work and the results reported by Aghakhani et al. [40]. This comparison is done for three-volume flow rates and the maximum error was 7.5% by experimental work and 0.9% by numerical work.

3. Results and discussion

It should be pointed out that the pin diameter is 2.5, the pin distance is 12.5, and the pin length is 12.5 if these parameters are not mentioned in the text.

3.1. Contours for different parameter ranges

Fig. 4 illustrates the temperature contours in a horizontal cross-section of a HEK by changing pin diameter, pin distance, and pin length. The temperature of the nanofluid from the inlet to the outlet is enhanced symmetrically from different angles in the HEK by increasing the radius and distance from the center of the HEK. Contact with hot pins causes the temperature of the nanofluid to rise in different parts. The pins are at different temperatures in the radial direction of the HEK, but they are symmetrical in temperature relative to each other in the angle direction. Inner pins are at lower temperatures and outer ones are at higher temperatures. The inner ones have better HTF due to the contact of nanofluid with the colder pins, and as a result, they have a lower temperature. The change in the dimensions of the pins and their distance has a great impact on their temperature. Also, the temperature of the nanofluid is changed by changing the dimensions of the pins and their distance. Pins with larger dimensions are at a higher temperature and the fluid around them is also at a higher temperature. The enlargement of the pins causes the contact surface of the pin and the nanofluid to enhance, leading to an increment in the temperature of the nanofluid in the parts where it collides with the pins. When the diameter of the pins is small, their temperature is greatly reduced and becomes close to the temperature of the nanofluid. By enhancing their diameter, their temperature becomes more different from the nanofluid and hotter pins are seen in the HEK, indicating more HTF from the bottom of the HEK to the pins.

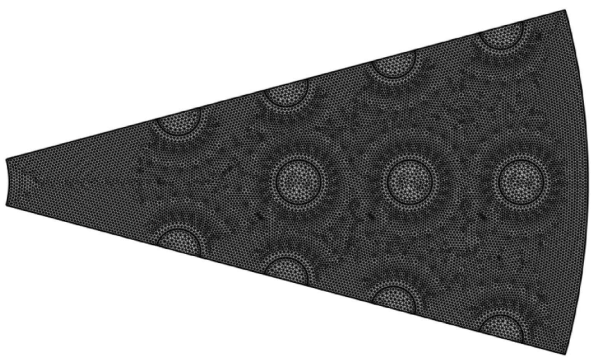

Fig. 3. A schematic of the grid for a part of the HEK geometry.

Table 3
Temperature values of the water in the copper HEK obtained from the present work and the results reported by Aghakhani et al. [40] for three-volume flow rates.

Volumetric flow rate (mL/min)	40	100	160
Present work	46.3 °C	39.6 °C	34.8 °C
Aghakhani et al. [40] (Experimental)	50.1 °C	42.6 °C	35.6 °C
Error%	7.5	7.0	2.2
Aghakhani et al. [40] (Simulation)	46.6 °C	39.8 °C	34.5 °C
Error%	0.6	0.5	0.9

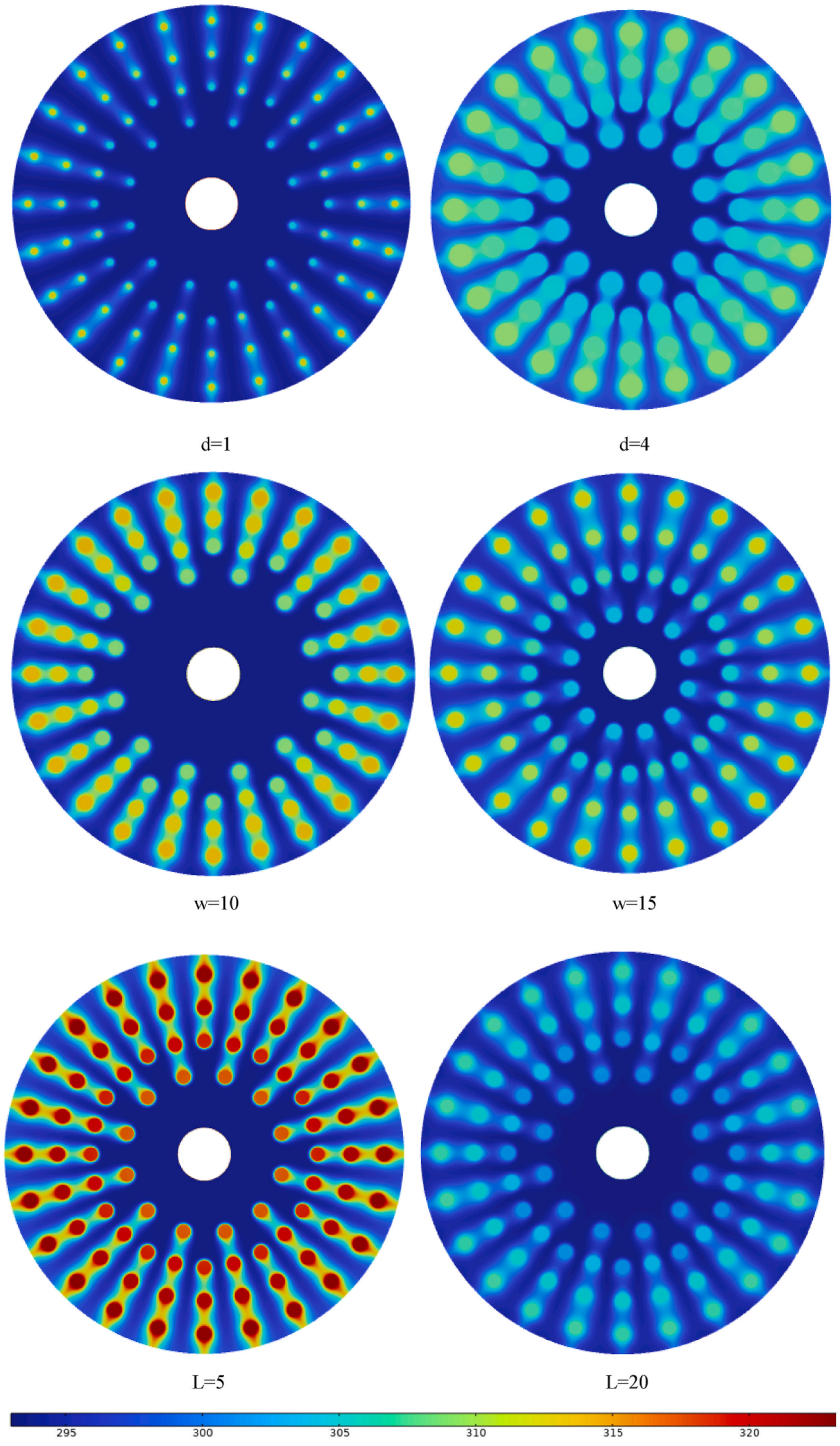

Fig. 4. Temperature contours (Kelvin) in a horizontal cross-section of a mid of the HEK by changing pin diameter, pin distance, and pin length (including nanofluid and solid part).

Fig. 5 depicts the temperature contours in the HEK by changing pin diameter, pin distance, and pin length in the absence of nanofluid. The temperature changes of the pins and HEK bottom are compared in this figure. In some cases, the temperatures of the pins and the bottom of the HEK are close to each other, and in other cases, the temperature of the pins is different from the temperature of the bottom of the HEK. In the case where the diameter of the pins is small, the temperature difference between the pins and the bottom of the HEK is high and the pins are much cooler than the bottom of the HEK. As the diameter of the pins is enhanced, the temperature of the pins becomes closer to the temperature of the bottom of the HEK and their temperature changes are close to each

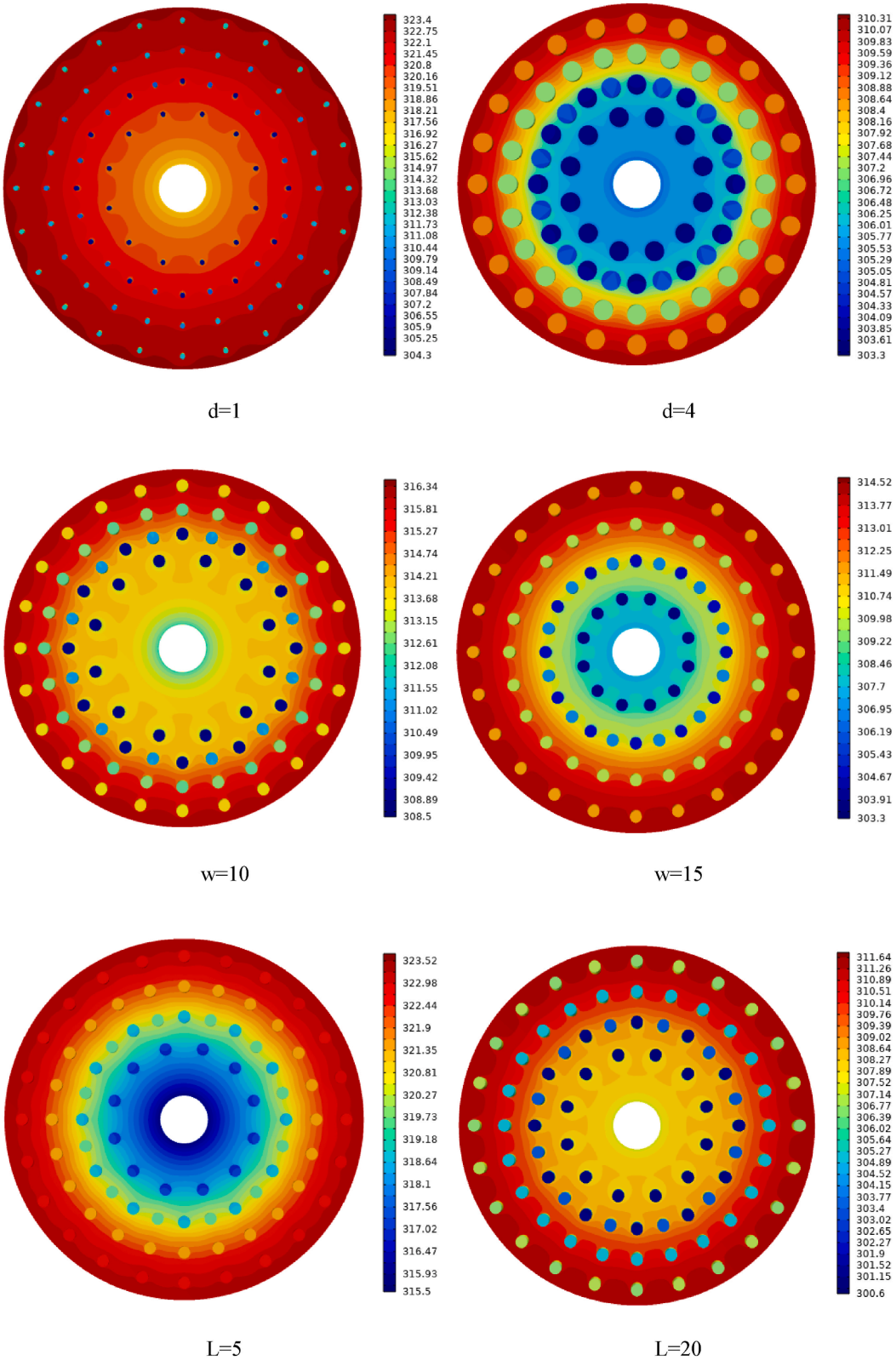

Fig. 5. Temperature contours (Kelvin) in the HEK by changing pin diameter, pin distance, and pin length in the absence of nanofluid (just solid part).

other. In the case where the pins are larger in diameter, the temperatures of the pins and the bottom of the HEK become closer to each other due to better HTF from the bottom of the HEK to the pins. In the case where the pins are further apart, the temperature of the pins and the bottom of the HEK is closer to each other, and in the case where the pins are placed at the HEK outlet, the temperature of the pins is lower than that of the bottom of the HEK. Less amount of HTF from the bottom of the HEK to the pins causes the temperature of the pins to reduce, but the bottom of the HEK is still at a higher temperature. In the case where the height of the pins is small, the temperature of the HEK bottom and the pins becomes closer. As the height of the pins is enhanced, there is a difference between the temperature of the pins and the bottom of the HEK. In the case where the pins are short, the tips of the pins are close to their bottoms so that their temperature is close to each other. By increasing the height of the pins, their end parts are cooled better and the lower parts still have a higher temperature, resulting in the temperature of the bottom of the HEK and the tip of the pins being different. It can be seen that the HEK with short pins has a higher temperature compared to the one with longer pins.

Fig. 6 demonstrates the temperature contours for an external view of the HEK by changing pin diameter, pin distance, and pin length in the absence of nanofluid. The temperature of the HEK and the nanofluid depends on the dimensions of the pins, their height and diameter, and their distance. The temperature changes in the nanofluid depend on the dimensions and distance of the pins because parts of the nanofluid are in contact with the pins and their temperature is increased. It can be seen that in the parts where the pins are installed, the temperature of the nanofluid in the middle parts behind the pins along the HEK radius is high. The changes in the dimensions of the pins and their distance affect the maximum temperature in the HEK. In some cases, the temperature of the HEK, especially the pins, is closer to the temperature of the nanofluid, but in some other cases, there is a temperature difference between them. In the case where the diameter of the pins is small, the temperature of the pins tends to the temperature of the nanofluid, but in the case of the pins with large diameters, the temperature of the pins is higher than that of the nanofluid. In this case, the temperature of the nanofluid is higher due to the collision with the hot surface. Distancing the pins from each other and arranging them in the entire HEK causes the temperature of the nanofluid to enhance between the pins and a hotter fluid exits from the HEK. In the case where the height of the pins is small, a little fluid passes over the HEK. However, as the height of the pins is intensified, more fluids pass over the HEK. Due to the entry of the constant nanofluid flow rate in two cases, the nanofluid velocity is slightly lower in the case where the height of the pins is higher. In the case that the height of the pins is lower, the nanofluid passes over the HEK with a higher velocity. It can be seen that the enhancement in the height of the pins reduces the temperature of the HEK.

Fig. 7 shows the temperature contours on the solid parts of the HEK and the nanofluid flow path with temperature coloring by changing pin diameter, pin distance, and pin length in the absence of nanofluid. In the vertical part of the HEK, the fluid covers the entire surface of the HEK. The fluid's path changes as it gets closer to the pins so that it may go through them and out of the outlet. Due to the continual increase in the cross-sectional area, a certain amount of velocity is lowered when moving the nanofluid in the radial direction of the HEK. The decrease in the cross-sectional area causes the nanofluid's velocity to rise as it approaches and travels past the edge of the pins. The temperature of the pins and nanofluid at the HEK output increases as the pins' diameter increases. The temperature of the nanofluid at the output is likewise increased by increasing the distance between the pins. The temperature of the pins rises as their height does. The movement of the nanofluid between the pins shows well in which parts the nanofluid has had more contact with the heatsink and in which parts the nanofluid has passed less due to the presence of a low-pressure area behind the pins.

3.2. Graphs for different parameter ranges

Fig. 8 illustrates the nanofluid pressure drop in the HEK by changing pin diameter, pin distance, and pin length in the absence of nanofluid. Although increasing the length increases the heat transfer, as seen in the figure and also seen in the study of Metzger et al. [26], it increases the pressure drop. Due to the small dimensions of the HEK and the low velocity of the nanofluid, the pressure drop in the HEK is small. However, changing the diameter and width of the pins, the distance between the pins has a great impact on the pressure drop. It can be seen that the increment in the diameter of the pins enhances the pressure drop in the HEK because as the pins' diameter is enhanced, they become closer. This causes the pressure drop in the HEK to enhance. An increment in the distance between the pins intensifies the pressure drop in the HEK. As the distance between the pins is increased, the pins are distributed in all parts of the HEK, leading to the nanofluid in most parts of the HEK passing through the pins. This causes the pressure drop in the HEK to enhance. Enhancing the height of the pins reduces the pressure drop in the HEK. As the height of the pins is intensified, the height of the HEK is increased. Due to the constant flow rate of the nanofluid, the nanofluid passes through the HEK more easily in a larger space, which causes a pressure drop. Therefore, the maximum HEK pressure drop, which is equal to 0.94 Pa, occurs for the shortest height of the pins, the largest distance between them, and the largest value of the diameter of the pins. The minimum value of the pressure drop, which was equal to 0.0004 Pa, occurs for the shortest and thinnest pins and smallest distance.

Fig. 9 demonstrates the variations of the HTC in the HEK by changing pin diameter, pin distance, and pin length. According to the study of Metzger et al. [26], increasing the length increases the heat transfer, and the same result was obtained in this study. The increase in the diameter of the pins causes the HTC between the nanofluid and the pins to enhance. By thickening the pins, the amount of HTF from the HEK to the nanofluid is increased, enhancing the HTC. The enhancement in the distance between the pins improves the HTC. By spacing the pins, the nanofluid passes better between them, the HTF is increased and the HTC is enhanced. But, the increase in the length of the pins significantly reduces the HTF rate. As the height of the pins is enhanced, the velocity in the HEK is decreased, which causes the HTC between the pins and the nanofluid to reduce. Therefore, the maximum value of the HTC between nanofluid and HEK, which is 344.17 $W/m^2.K$, occurs for the large diameter of the pins, their greater distance from each other, and the lower height of the pins. The minimum value, which is 49.85 $W/m^2.K$, corresponds to the smallest diameter and distance of the pins when the distance between the pins is 18.2.

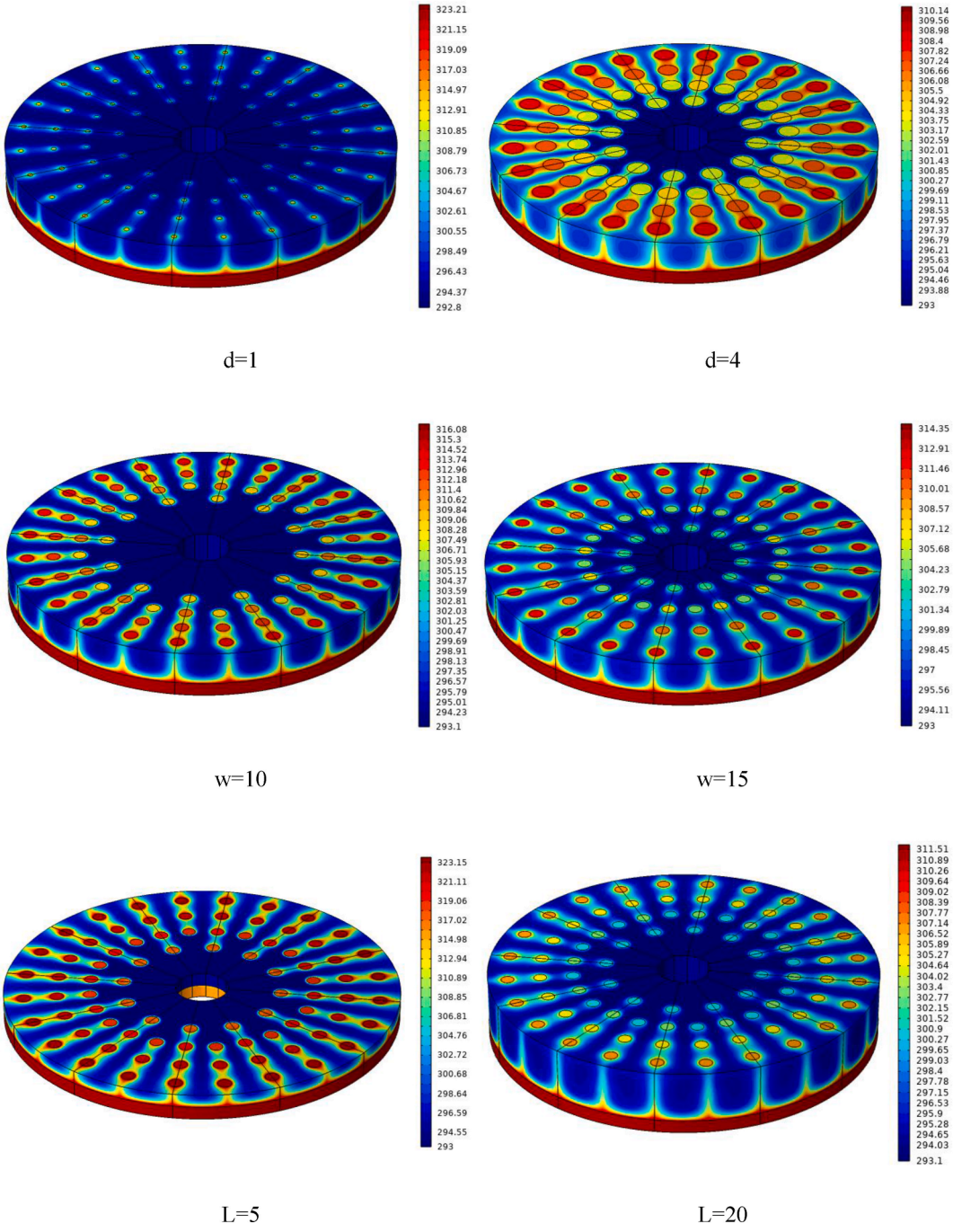

Fig. 6. Temperature contours (Kelvin) for an external view of the HEK by changing pin diameter, pin distance, and pin length.

Fig. 10 illustrates the heatsink THR changes by changing pin diameter, pin distance, and pin length. An increment in the diameter of the pins greatly affects the THR of the HEK and reduces it significantly. By increasing the diameter of the pins, the contact surface between the nanofluid and the pins is enhanced and the heat is better transferred from the HEK bottom to the nanofluid, leading to a reduction in the heatsink THR. The enhancement in the height of the pins decreases the THR of the HEK. As the length of the pins is enhanced, more heat is transferred from the HEK to the nanofluid due to the increase in the contact surface. The increase in the distance between the pins has a slight effect on the THR compared to the other two parameters. It can be seen that the THR is reduced with the distance between the pins. The easier flow of the nanofluid between the pins reduces the temperature of the HEK and reduces its resistance. The minimum value of THR, which is 0.0001 K/W, occurs in the longest and thickest pins and largest distance from each other. The maximum THR, which is 0.0005 K/W, corresponds to the smallest pins and the shortest distance between pins.

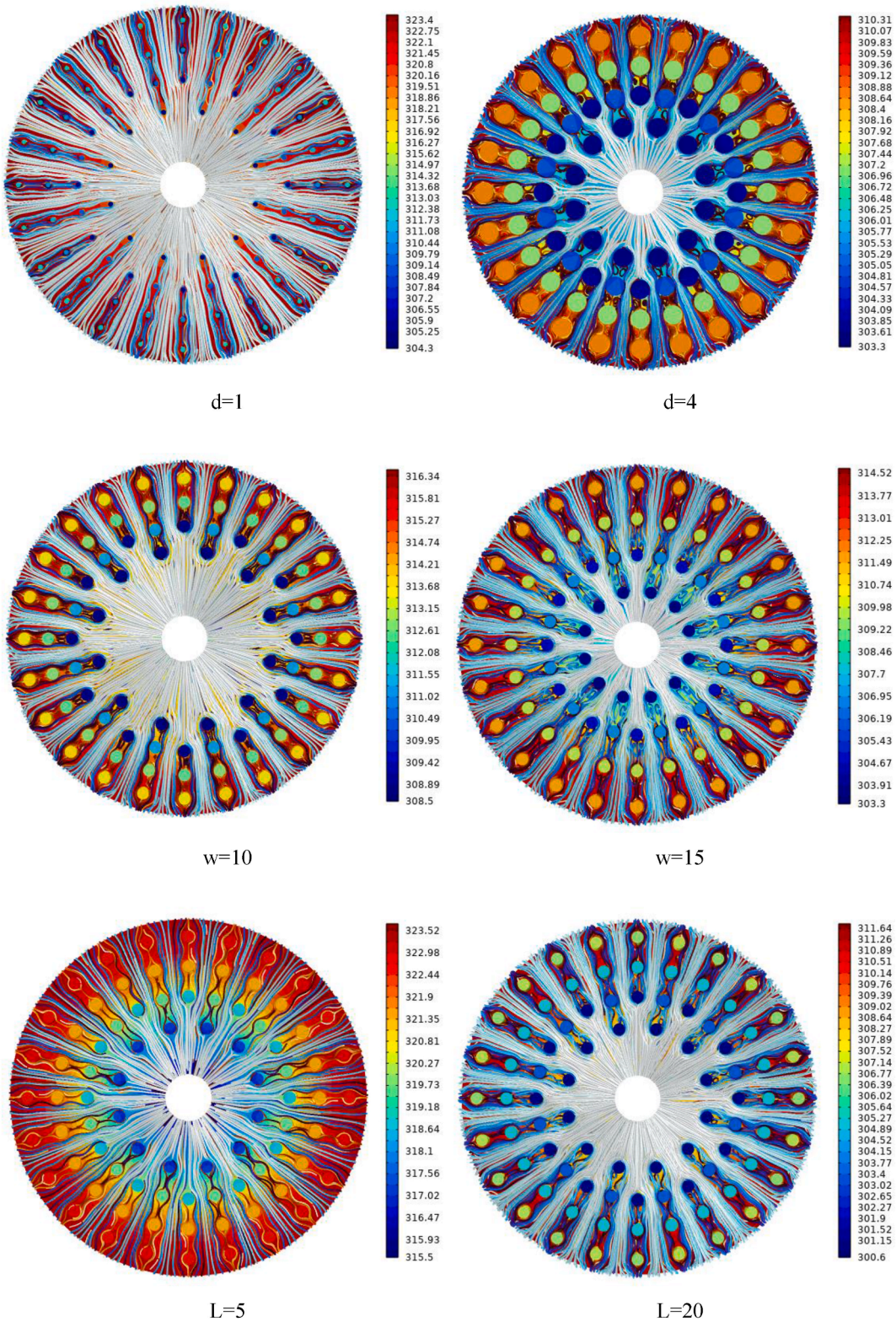

Fig. 7. Temperature contours (Kelvin) on the solid parts of the HEK and the nanofluid flow path with temperature coloring by changing pin diameter, pin distance, and pin length.

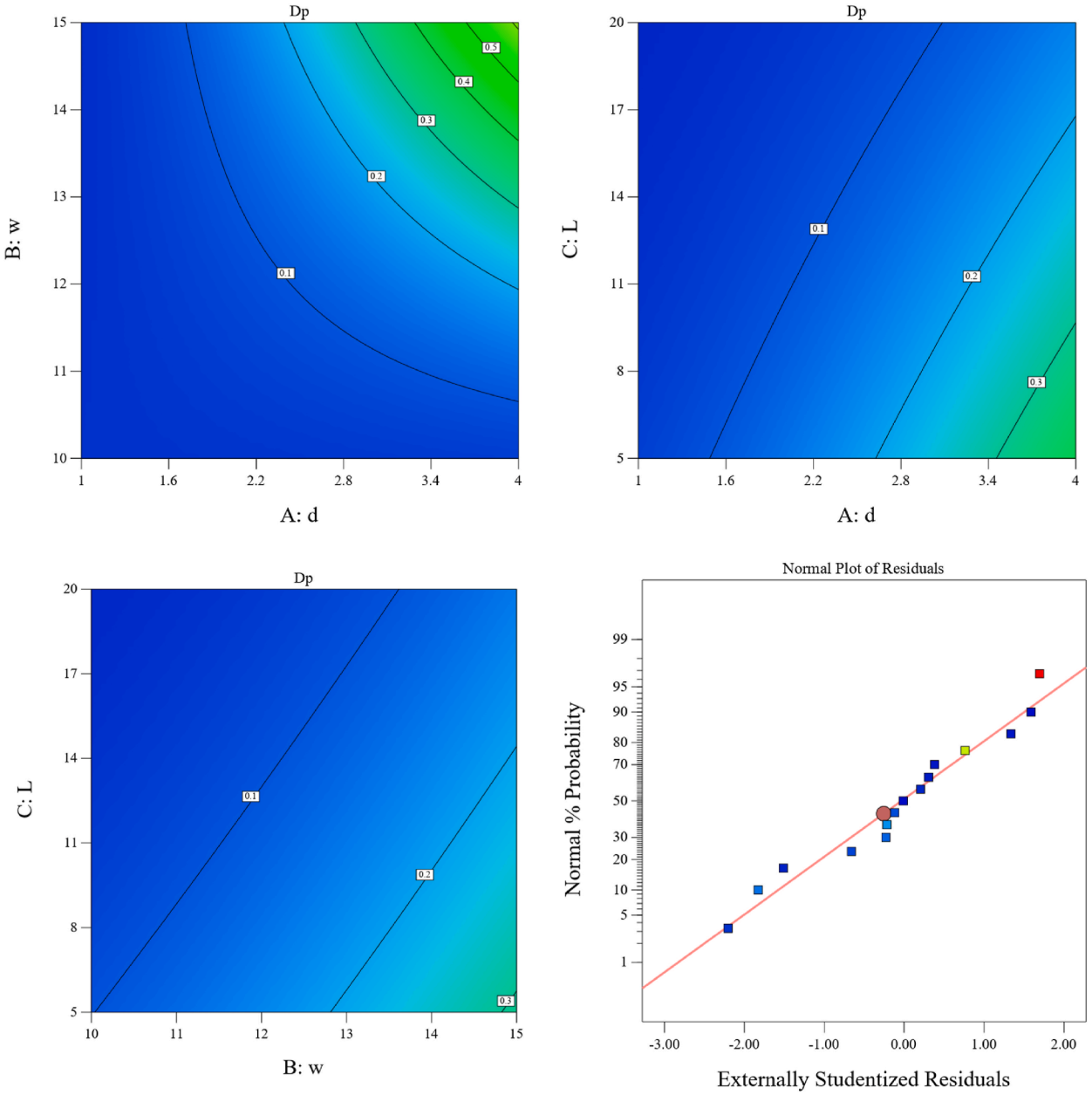

Fig. 8. Nanofluid pressure drop in the HEK by changing pin diameter, pin distance, and pin length.

Fig. 11 shows the variations of Teta on the HEK bottom by changing pin diameter, pin distance, and pin length. Temperature uniformity refers to the distribution of temperature in a certain region or system. In a system with good temperature uniformity, all points or regions experience similar or identical temperatures. This is important in various applications, especially in thermal management and heat dissipation monitoring, to ensure performance, reliability, and safety. Poor temperature uniformity can lead to uneven heat distribution thereby producing hot spots, reduced performance, or potential component damage in electronic devices. Therefore, this issue is discussed in this section. The purpose of checking this parameter is to achieve temperature uniformity and maintain optimal thermal conditions in this type of heat sink. Pin length, pin spacing, and pin diameter are important parameters that affect heat sink temperature uniformity. Longer and thicker pins generally increase the surface area for heat dissipation. This can increase the overall cooling capacity of the heatsink and contribute to better temperature uniformity. However, longer and thicker pins also increase airflow resistance and affect cooling efficiency. Increasing the value of the diameter of the pin caused the value of Teta to decrease, which meant an increase in uniformity on the HEK. Better heat transmission from the HEK's bottom to the pins results from an increase in the pins' diameter. As a result, the nanofluid can cool it more effectively and lower the HEK's temperature range between the maximum and minimum. The same outcome is obtained with a pin length in-

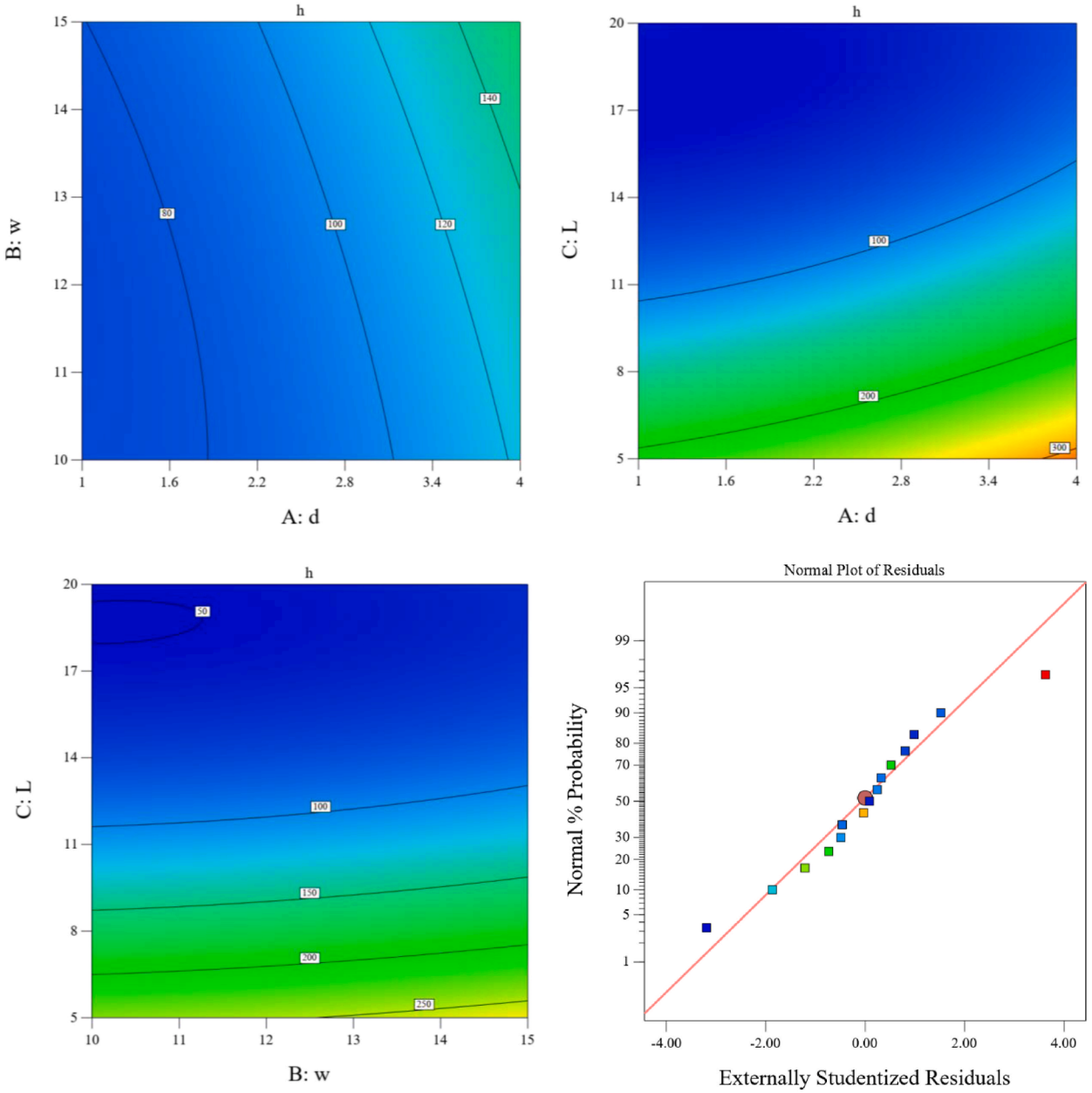

Fig. 9. Variations of the HTC in the HEK by changing pin diameter, pin distance, and pin length.

crease. Teta is decreased by increasing the space between the pins. Better distribution of the pins on the HEK bottom leads to the temperature becoming more uniform and Teta being decreased. The best Teta corresponds to the thickest and longest pins at a large distance. Reducing the dimensions of the pins as well as the distance between them enhances Teta in the HEK.

4. Conclusions

This article analyzes a new-design HEK numerically using the FEM. Several circular pin fins are placed in the HEK. The values of pressure drop, Teta, THR, and HTC are estimated by changing their diameter and height, as well as their distance using machine learning. Nanofluid flows inside the HEK. The results demonstrate.

1 The best Teta corresponds to the thickest and longest pins at a large distance. Reducing the dimensions of the pins as well as the distance between them enhances Teta in the HEK.
2 The minimum value of THR, which is 0.0001 K/W, occurs in the longest and thickest pins and largest distance from each other. The maximum THR, which is 0.0005 K/W, corresponds to the smallest pins and the shortest distance between pins.

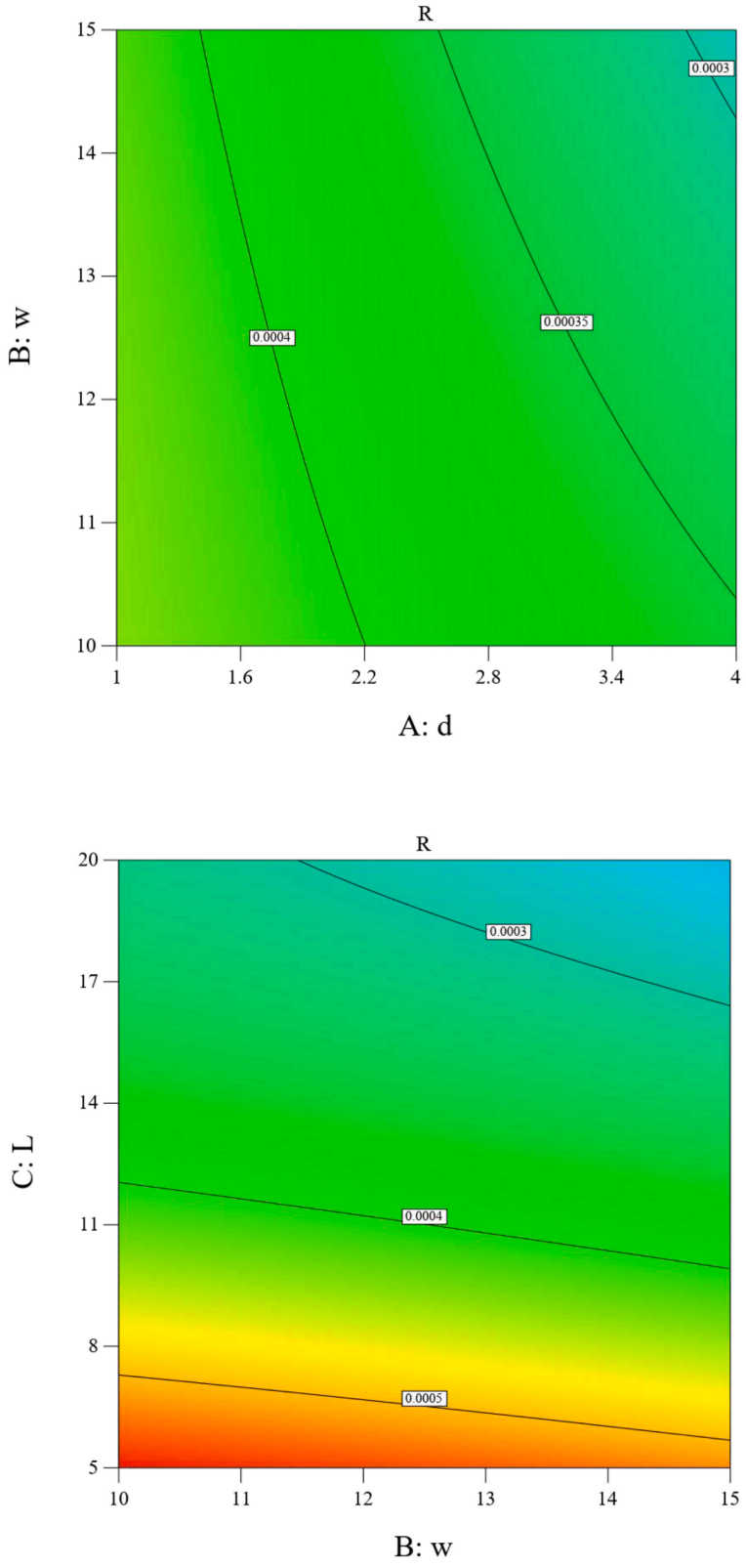

Fig. 10. Heatsink THR changes by changing pin diameter, pin distance, and pin length.

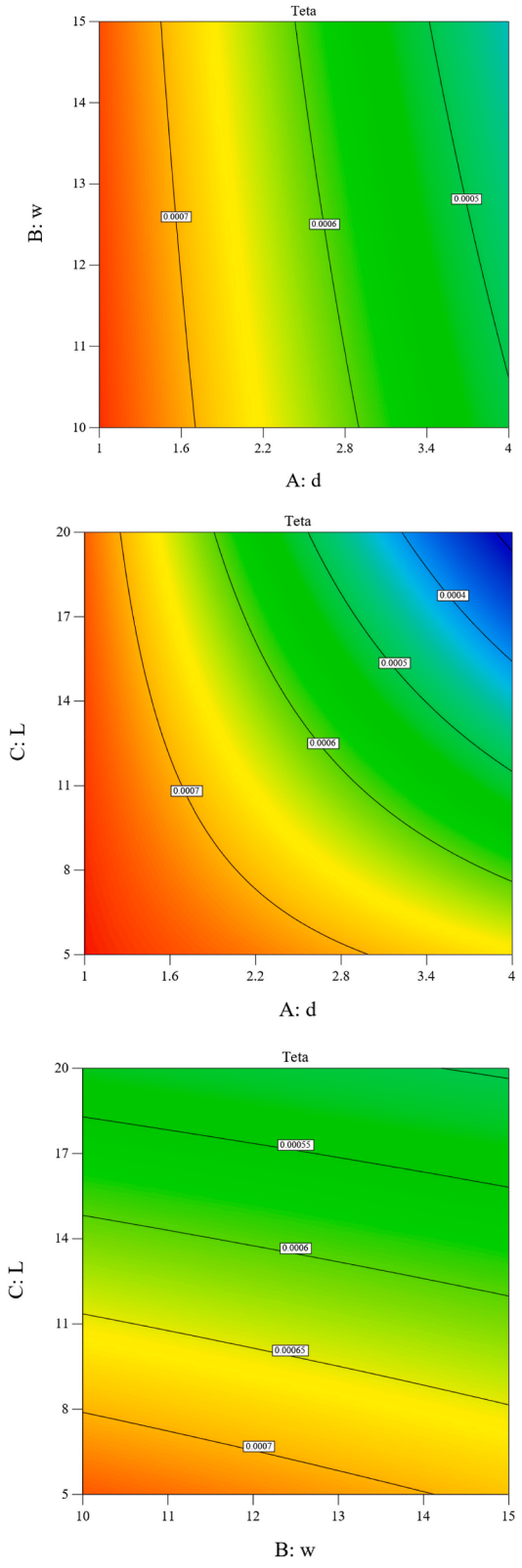

Fig. 11. Variations of Temperature uniformity on the HEK bottom by changing pin diameter, pin distance, and pin length.

3 The maximum value of the HTC between nanofluid and HEK, which is 344.17 W/m^2.K, occurs for the large diameter of the pins, their greater distance from each other, and the lower height of the pins. The minimum value, which is 49.85 W/m^2.K, corresponds to the smallest diameter and distance of the pins when the distance between the pins is 18.2. With the increase in the diameter of the pins, it can be seen that the value of HTC has increased by 40.4% for the shortest distance and the shortest length, while it has increased by 59.47% for the longest distance and the shortest length. Also, the lowest reduction of HTC with increasing pin length in the smallest diameter and the smallest distance was 76.11%.
4 The maximum HEK pressure drop, which is equal to 0.94 Pa, occurs for the shortest height of the pins, the largest distance between them, and the largest value of the diameter of the pins. The minimum value of the pressure drop, which was equal to 0.0004 Pa, occurs for the shortest and thinnest pins and smallest distance.
5 Increasing the diameter of the pins at their minimum distance increases the pressure drop up to 56.67%, while at the maximum distance between the pins, the pressure drop increases up to 90.63%.

5. Recommendations

Considering that the flow of Newtonian nanofluids has been investigated in this study, non-Newtonian nanofluids or hybrid nanofluids can be used for future studies.

It is possible to check and predict operational parameters using machine learning and compare its results with laboratory results.

Turbulent flow can be investigated with different models on this geometry and this investigation can be done at much larger Reynolds numbers.

Different pin shapes can be analyzed and compared numerically and experimentally.

CRediT authorship contribution statement

Behzad Heidarshenas: Writing – original draft, Software, Methodology. **Awatef Abidi:** Writing – review & editing. **S. Mohammad Sajadi:** Writing – review & editing. **Yanjie Yuan:** Validation, Methodology, Investigation. **A.S. El-Shafay:** Writing – review & editing, Software. **Hikmet Ş. Aybar:** Supervision, Investigation.

Declaration of competing interest

The authors declare that they have no known competing financial interests or personal relationships that could have appeared to influence the work reported in this paper.

Data availability

No data was used for the research described in the article.

Acknowledgments

The second author (Awatef Abidi) extends her appreciation to the Deanship of Scientific Research at King Khalid University for funding this work through the Large Groups Project under grant number (R.G.P.2/204/44).

References

[1] B. Rajabifar, Enhancement of the performance of a double layered microchannel heatsink using PCM slurry and nanofluid coolants, Int. J. Heat Mass Tran. 88 (2015) 627–635.
[2] M. Lossec, B. Multon, H. Ben Ahmed, Sizing optimization of a thermoelectric generator set with heatsink for harvesting human body heat, Energy Convers. Manag. 68 (2013) 260–265.
[3] Y. Jiang, X. Wang, M.Z. Mahmoud, M.A. Elkotb, L. Baloo, Z. Li, B. Heidarshenas, A study of nanoparticle shape in water/alumina/boehmite nanofluid flow in the thermal management of a lithium-ion battery under the presence of phase-change materials, J. Power Sources 539 (2022) 231522.
[4] F. Dilbaz, F. Selimefendigil, H.F. Öztop, Lithium-ion battery module performance improvements by using nanodiamond-FE_3O_4 water/ethylene glycol hybrid nanofluid and fins, J. Therm. Anal. Calorim. 147 (2022) 10625–10635, https://doi.org/10.1007/s10973-022-11269-9.
[5] S. Saleem, B. Heidarshenas, An investigation on exergy in a wavy wall microchannel heat sink by using various nanoparticles in fluid flow: two-phase numerical study, J. Therm. Anal. Calorim. 145 (2021) 1599–1610, https://doi.org/10.1007/s10973-021-10771-w.
[6] L. Ben Said, L. Kolsi, N. Ben Khedher, F. Alshammari, E.H. Malekshah, A.K. Hussein, Numerical study of the fluid-structure interaction during CNT-water nanofluid mixed convection in a micro-channel equipped with elastic fins under periodic inlet velocity conditions, Exp. Tech. 47 (2023) 7–15.
[7] M.U. Sajid, H.M. Ali, Recent advances in application of nanofluids in heat transfer devices: a critical review, Renew. Sustain. Energy Rev. 103 (2019) 556–592.
[8] M. Ibrahim, S. Saleem, YM. Chu, et al., An investigation of the exergy and first and second laws by two-phase numerical simulation of various nanopowders with different diameter on the performance of zigzag-wall micro-heat sink (ZZW-MHS), J. Therm. Anal. Calorim. 145 (2021) 1611–1621, https://doi.org/10.1007/s10973-021-10786-3.
[9] S. Rostami, A.A. Nadooshan, A. Raisi, M. Bayareh, Effect of using a heatsink with nanofluid flow and phase change material on thermal management of plate lithium-ion battery, J. Energy Storage 52 (2022) 104686.
[10] Y. Alihosseini, M. Zabetian Targhi, M.M. Heyhat, N. Ghorbani, Effect of a micro heat sink geometric design on thermo-hydraulic performance: a review, Appl. Therm. Eng. 170 (2020) 114974.
[11] M. Ghaneifar, H. Arasteh, R. Mashayekhi, A. Rahbari, R. Babaei Mahani, P. Talebizadehsardari, Thermohydraulic analysis of hybrid nanofluid in a multilayered copper foam heat sink employing local thermal non-equilibrium condition: optimization of layers thickness, Appl. Therm. Eng. 181 (2020) 115961.
[12] Y.-M. Chu, M. Ibrahim, T. Saeed, A.S. Berrouk, E.A. Algehyne, R. Kalbasi, Examining rheological behavior of MWCNT-TiO2/5W40 hybrid nanofluid based on experiments and RSM/ANN modeling, J. Mol. Liq. 333 (2021) 115969.
[13] H. Yu, B. Duan, L. Feng, R. Kalbasi, Thermophysical properties improvement of a common liquid by adding reduced graphene oxide: an experimental study, Powder Technol. 384 (2021) 466–478.
[14] S. Kumar, A. Kumar, A. Darshan Kothiyal, M. Singh Bisht, A review of flow and heat transfer behaviour of nanofluids in micro channel heat sinks, Therm. Sci.

Eng. Prog. 8 (2018) 477–493.
[15] M.M. Tafarroj, O. Mahian, A. Kasaeian, K. Sakamatapan, A.S. Dalkilic, S. Wongwises, Artificial neural network modeling of nanofluid flow in a microchannel heat sink using experimental data, Int. Commun. Heat Mass Tran. 86 (2017) 25–31.
[16] F.M. Allehiany, E.E. Mahmoud, S. Berrouk, V. Ali, M. Ibrahim, Evaluating the efficiency of pin–fin micro-heat sink considering different shapes of nanoparticle based on exergy analysis, J. Therm. Anal. Calorimetry 145 (2021) 1623–1632.
[17] D. Metzger, R. Berry, J. Bronson, Developing Heat Transfer in Rectangular Ducts with Staggered Arrays of Short Pin Fins, 1982.
[18] D. Lelea, The tangential micro-heat sink with multiple fluid inlets, Int. Commun. Heat Mass Tran. 39 (2012) 190–195.
[19] J. Choi, M. Jeong, J. Yoo, M. Seo, A new CPU cooler design based on an active cooling heatsink combined with heat pipes, Appl. Therm. Eng. 44 (2012) 50–56.
[20] S.S. Khaleduzzaman, M.R. Sohel, R. Saidur, I.M. Mahbubul, I.M. Shahrul, B.A. Akash, J. Selvaraj, Energy and exergy analysis of alumina–water nanofluid for an electronic liquid cooling system, Int. Commun. Heat Mass Tran. 57 (2014) 118–127.
[21] A. Mohammed Adham, N. Mohd-Ghazali, R. Ahmad, Thermal and hydrodynamic analysis of microchannel heat sinks: a review, Renew. Sustain. Energy Rev. 21 (2013) 614–622.
[22] D. Metzger, Z. Fan, W. Shepard, Pressure loss and heat transfer through multiple rows of short pin fins, in: International Heat Transfer Conference Digital Library, Begel House Inc., 1982.
[23] G. Steuber, D. Metzger, Heat transfer and pressure loss performance for families of partial length pin fin arrays in high aspect ratio rectangular ducts, in: International Heat Transfer Conference Digital Library, Begel House Inc., 1986.
[24] D. Metzger, W. Shepard, S. Haley, Row resolved heat transfer variations in pin-fin arrays including effects of non-uniform arrays and flow convergence, in: Turbo Expo: Power for Land, Sea, and Air, vol. 79313, American Society of Mechanical Engineers, 1986 V004T009A015.
[25] P. Bhandari, K.S. Rawat, Y.K. Prajapati, D. Padalia, L. Ranakoti, T. Singh, Design modifications in micro pin fin configuration of microchannel heat sink for single phase liquid flow: a review, J. Energy Storage 66 (2023) 107548.
[26] D. Metzger, C. Fan, S. Haley, Effects of Pin Shape and Array Orientation on Heat Transfer and Pressure Loss in Pin Fin Arrays, 1984.
[27] D. Metzger, S. Haley, Heat Transfer Experiments and Flow Visualization for Arrays of Short Pin Fins, American Society of Mechanical Engineers, 1982.
[28] X. Yu, J. Feng, Q. Feng, Q. Wang, Development of a plate-pin fin heat sink and its performance comparisons with a plate fin heat sink, Appl. Therm. Eng. 25 (2005) 173–182.
[29] H.A. Hussein, Numerical hydrothermal evaluation of heat transfer in a multi-mini-channel heat sink: effect of square pin fins, Results in Engineering 20 (2023) 101403.
[30] A.H. Pordanjani, A. Raisi, A. Daneh-Dezfuli, Slip and non-slip flows of MHD nanofluid through microchannel to cool discrete heat sources in presence and absence of viscous dissipation, J. Magn. Magn Mater. 580 (2023) 170972.
[31] A. Akbarinia, R. Laur, Investigating the diameter of solid particles effects on a laminar nanofluid flow in a curved tube using a two phase approach, Int. J. Heat Fluid Flow 30 (2009) 706–714.
[32] A. Akbarinia, A. Behzadmehr, Numerical study of laminar mixed convection of a nanofluid in horizontal curved tubes, Appl. Therm. Eng. 27 (2007) 1327–1337.
[33] J. Xu, A. Rouelle, K.M. Smith, D. Celik, M.Y. Hussaini, S.W. Van Sciver, Two-phase flow of solid hydrogen particles and liquid helium, Cryogenics 44 (2004) 459–466.
[34] L. Schiller, A drag coefficient correlation, J Zeit. Ver. Deutsch. Ing. 77 (1933) 318–320.
[35] K. Khanafer, K. Vafai, M. Lightstone, Buoyancy-driven heat transfer enhancement in a two-dimensional enclosure utilizing nanofluids, Int. J. Heat Mass Tran. 46 (2003) 3639–3653.
[36] N. Masoumi, N. Sohrabi, A. Behzadmehr, A new model for calculating the effective viscosity of nanofluids, J. Phys. Appl. Phys. 42 (2009) 055501.
[37] C.H. Chon, K.D. Kihm, S.P. Lee, S.U.S. Choi, Empirical correlation finding the role of temperature and particle size for nanofluid (Al2O3) thermal conductivity, enhancement 87 (2005) 153107.
[38] S.M. Vahedi, S. Aghakhani, A.H. Pordanjani, J. Azaiez, A comprehensive parametric study on heat transfer optimization of a triangular enclosure subjected to a magnetic field using neural network machine learning, Eng. Anal. Bound. Elem. 145 (2022) 173–186.
[39] S.M. Vahedi, A.H. Pordanjani, A. Raisi, A.J. Chamkha, Sensitivity analysis and optimization of MHD forced convection of a Cu-water nanofluid flow past a wedge, Eur. Phys. J. Plus 134 (2019) 1–21.
[40] S. Aghakhani, A. Hajatzadeh Pordanjani, M. Afrand, A.K. Farsani, N. Karimi, M. Sharifpur, Entropy generation and exergy analysis of Ag–MgO/water hybrid nanofluid within a circular heatsink with different number of outputs, Int. J. Therm. Sci. 184 (2023) 107891.